J Musculoskelet Neuronal Interact 2026; 26(1):124-133

Journal of Musculoskeletal and Neuronal Interactions JMNI

Original Article

Targeting the STK39/ARID2 Axis to Inhibit NF-κB Signaling: A Novel Pathway for Mesenchymal Stem Cell Osteogenic Differentiation in Osteoporosis Management

Yang Wang[1], Dong Wei[1], Zhineng Chen[2], Liang Zhong[1]

[1]Department of Traditional Chinese Orthopedics, Hangzhou Xiaoshan District Traditional Chinese Medicine Hospital, Zhejiang, China; [2]Department of Traditional Chinese Orthopedics, The Third Affiliated Hospital of Zhejiang Chinese Medical University, Zhejiang, China

Abstract

Objectives: Osteoporosis (OP) is a prevalent bone disease characterized by reduced bone mass and increased fracture risk, in part due to impaired osteogenic differentiation of bone marrow–derived mesenchymal stromal cells (BMSCs). Loss of AT-rich interactive domain–containing protein 2 (ARID2) attenuates BMSC osteogenesis, but the underlying mechanism remains to be elucidated. **Methods**: Human BMSCs were induced to undergo osteogenic or adipogenic differentiation. Lentiviral transduction was used to silence ARID2 and/or overexpress serine/threonine kinase 39 (STK39). Effects on BMSC fate were assessed by quantitative reverse-transcription PCR (qRT-PCR), MTT assay, alkaline phosphatase (ALP) staining, Alizarin Red S (ARS) staining, Oil Red O staining, and western blotting. **Results**: ARID2 expression increased over time during osteogenic induction. ARID2 silencing reduced BMSC proliferation and osteogenic differentiation while favoring adipogenesis. Conversely, STK39 overexpression enhanced proliferation and osteogenic differentiation and attenuated nuclear factor κB (NF-κB) signaling during osteogenic induction; these effects were reversed by ARID2 silencing. **Conclusion**: The STK39–ARID2 axis promotes osteogenic differentiation and suppresses adipogenic differentiation of BMSCs, at least in part via inhibition of NF-κB signaling. These findings highlight a potential molecular target for therapeutic strategies in OP.

Keywords: AT-rich interactive domain-containing protein 2, Bone marrow mesenchymal stem cells, Osteogenic differentiation, Osteoporosis, Serine/threonine kinase 39

Introduction

Osteoporosis (OP) is a chronic metabolic bone disease characterized by decreased bone density and disrupted bone microarchitecture, resulting in increased fracture risk and contributing substantially to morbidity and mortality in older adults[1]. Current therapies for OP include bisphosphonates, denosumab, teriparatide, abaloparatide, romosozumab, and selective estrogen receptor modulators[1], all of which aim to prevent fractures by either reducing bone resorption or promoting bone formation[2].

Bone marrow–derived mesenchymal stromal cells (BMSCs) are multipotent stromal cells with self-renewal capacity and multilineage differentiation potential[3]. Under osteogenic induction, BMSCs differentiate into osteoblasts that deposit mineralized bone matrix and support bone formation[4]. Dysregulated BMSC differentiation is implicated in OP: osteogenic differentiation is attenuated, whereas adipogenic commitment is favored, leading to reduced bone formation and increased marrow adipose tissue[5,6]. Given the potential adverse effects associated with long-term pharmacologic therapy[5], contemporary research on OP increasingly focuses on molecular mechanisms underlying the osteo-adipogenic imbalance in mesenchymal stromal cells (MSCs) and marrow adipose tissue[7].

STK39, also known as SPAK, is a STE20/SPS1-related proline/alanine-rich kinase that contains a putative nuclear localization signal and a caspase-cleavage site separating

The authors have no conflict of interest.

Corresponding author: Liang Zhong, Department of Traditional Chinese Orthopedics, Hangzhou Xiaoshan District Traditional Chinese Medicine Hospital, No. 156 Yucai Road, Hangzhou 311201, Zhejiang, China
E-mail: tfqskvfwner@hotmail.com • 15824102079@163.com

Edited by: G. Lyritis
Accepted 1 December 2025

Table 1. Primers used in quantitative reverse-transcription polymerase chain reaction.

Genes	Species	Amplicon size (bp)	Primer sequence (5'-3')	
ARID2	human	167	Forward	CAGTGTGTCGGATTATCTGCG
			Reverse	GCATGACGTGCTTGCTTTCATT
STK39	human	84	Forward	TGCCAGACCAGTATGGATGAA
			Reverse	GGTGTAATAGGTCACTACGTTGG
GAPDH	human	197	Forward	GGAGCGAGATCCCTCCAAAAT
			Reverse	GGCTGTTGTCATACTTCTCATGG

the kinase and CCT domains. Full-length STK39 is diffusely distributed in unstimulated cells, whereas a truncated form generated by caspase cleavage accumulates in the nucleus[8]. Although direct evidence linking STK39 to osteogenic differentiation is lacking, STK39 has been implicated in cell differentiation (via Ste20-family signaling)[9] and in bone/mineral metabolism[10]. Notably, it has been reported to activate transforming growth factor-β1 (TGF-β1) signaling[11], which is abundant in the bone matrix and recruits BMSCs to promote osteogenic differentiation[4,12]. Thus, upregulation of STK39 may favor BMSC osteogenic differentiation and help mitigate OP pathology.

Furthermore, sustained activation of pro-osteogenic bone morphogenetic protein (BMP)/TGF-β1 signaling induces expression of AT-rich interactive domain–containing protein 2 (ARID2) in BMSCs[13]. ARID2 encodes BAF200, a subunit of the polybromo-associated BAF (PBAF) chromatin-remodeling complex[14], which facilitates ligand-dependent transcriptional activation by nuclear receptors[15]. Deficiency of ARID2 leads to marked repression of osteolineage gene expression and impaired osteogenic differentiation in BMSCs[13]. Therefore, STK39 overexpression may promote BMSC osteogenesis in a manner consistent with a model in which TGF-β1 signaling upregulates ARID2, although TGF-β pathway activity was not directly measured in this study.

Nuclear factor κB (NF-κB) signaling is widely recognized as a negative regulator of osteogenesis, exerting an inhibitory effect on BMSC osteogenic progression[16]. NF-κB activation has also been implicated in adipogenic differentiation of BMSCs[17]. In other contexts, reduced ARID2 expression leads to NF-κB activation (e.g., cervical cancer)[18]. Accordingly, elevation of ARID2 expression by STK39 overexpression may facilitate BMSC osteogenesis and suppress adipogenesis by attenuating NF-κB signaling. In this study, *in vitro* cellular experiments combined with molecular assays were performed to evaluate whether this mechanism operates in BMSCs, with potential implications for targeted therapy in OP.

Materials and Methods

Cell culture

The human BMSC line UE6E7T-1 was obtained from the Japanese Collection of Research Bioresources (JCRB) Cell Bank (JCRB1131; Osaka, Japan). UE6E7T-1 is an immortalized BMSC line generated by retroviral transduction with human papillomavirus type 16 (HPV16) E6/E7 and human telomerase reverse transcriptase (hTERT) (JCRB1131 record)[19]. Cells were maintained in MesenCult Human MSC Basal Medium (05401; STEMCELL Technologies, Vancouver, Canada) at 37°C in a humidified atmosphere with 5% CO_2. Experiments were performed using cells between passages 4 and 8. Short tandem repeat (STR) authentication was performed within the last year to confirm cell-line identity, and mycoplasma testing was negative.

Osteogenic differentiation

BMSCs were grown to approximately 70% confluence and then transferred to DMEM (11885092; Thermo Fisher Scientific, Waltham, MA, USA) supplemented with 10% fetal bovine serum (FBS) (E600001; Sangon Biotech, Shanghai, China), penicillin–streptomycin (100 U/mL penicillin and 100 µg/mL streptomycin; 15140122; Thermo Fisher Scientific, USA), 2 mM L-glutamine, 0.25 mM ascorbic acid (A610021; Sangon Biotech, China), 10 mM β-glycerophosphate (G9422; Sigma-Aldrich, St. Louis, MO, USA), and 0.1 µM dexamethasone (D4902; Sigma-Aldrich, USA). Cells were cultured for 1, 3, 5, 7, and 14 days[13]. The medium was replaced every 2–3 days, and at each time point, qRT-PCR was performed to assess ARID2 expression.

Cell transduction

Lentiviral particles encoding ARID2 silencing (siARID2; TL306601) and STK39 overexpression (RC223981L4V), together with their corresponding negative controls (siNC; TR30023 and NC; PS100093), were obtained from OriGene (Rockville, MD, USA). BMSCs were allocated to the following groups: siNC, siARID2, NC + siNC, NC + siARID2, STK39 overexpression + siNC, and STK39 overexpression + siARID2. For transduction, 1×10^5 BMSCs were seeded per well in 24-well plates (growth area ~1.9 cm^2 per well; seeding density ~5.3×10^4 cells/cm^2) and cultured at 37°C for 24 h. Lentivirus was then added at a multiplicity of infection (MOI) of 25[20] in the presence of 8 µg/mL polybrene (S2667; Sigma-Aldrich, USA).

After 24 h of transduction, the medium was replaced

Table 2. Primary/secondary antibodies used in western blot.

Antibodies	Species	Molecular weight	Clones	Dilutions	Catalog numbers	Vendor
ARID2	Rabbit	197 kDa	BLR213K	1 μg/mL	ab314046	Abcam
p-p65	Rabbit	65 kDa	EP2294Y	1:1000	ab76302	Abcam
p65	Rabbit	65 kDa	EP2161Y	1:1000	ab76311	Abcam
IκBα	Rabbit	37 kDa	EPR5037	1:5000	ab109509	Abcam
GAPDH	Rabbit	36 kDa	EPR16891	1:200000	ab181602	Abcam
Secondary antibodies	Goat	—	—	1:5000	ab6721	Abcam

with fresh growth medium and cells were allowed to recover for 4 h. Cells were then subjected to osteogenic or adipogenic induction as indicated, and downstream assays were performed at the specified time points. Transduction efficiency was verified by qRT-PCR, and experiments proceeded when target gene silencing or overexpression was ≥90% relative to the corresponding control (siNC or vector NC).

qRT-PCR

With or without lentiviral transduction, BMSCs were lysed in TRIzol reagent (15596026; Thermo Fisher Scientific, USA) to isolate total RNA. cDNA was synthesized using the PrimeScript RT Reagent Kit (DRR037A; Takara, Dalian, China) according to the manufacturer's instructions. Quantitative real-time PCR was performed on a LightCycler 96 system (Roche, Indianapolis, IN, USA) under the cycling conditions recommended for Eastep qPCR Master Mix (LS2062; Promega, Madison, WI, USA). GAPDH served as the reference gene, and relative expression levels were calculated using the $2^{-\Delta\Delta Ct}$ method[21]. Primer sequences are provided in Table 1.

MTT assay

BMSCs were transduced as described and seeded in 96-well plates at 1×10^4 cells/well. After cells adhered (overnight), each well was incubated with 20 μL of 5 mg/mL MTT solution (ST316; 3-(4,5-dimethyl-2-thiazolyl)-2,5-diphenyl-2-H-tetrazolium bromide; Beyotime, Shanghai, China) for 4 h. The medium was then removed, and 150 μL dimethyl sulfoxide (DMSO) (34869; Sigma-Aldrich, USA) was added. Plates were agitated at ~50 rpm for 10 min to dissolve the formazan. Optical density (OD) was measured at 570 nm using a microplate reader (Synergy HTX; BioTek, Winooski, VT, USA).

Adipogenic differentiation and Oil Red O staining

BMSCs were transduced with or without lentiviruses silencing ARID2 and then induced to undergo adipogenic differentiation by replacing the medium of confluent cultures with DMEM containing 20% FBS, penicillin–streptomycin (100 U/mL penicillin and 100 μg/mL streptomycin), and 2 mM L-glutamine, supplemented with 0.1 μM dexamethasone, 100 μM β-mercaptoethanol (444203; Sigma-Aldrich, USA), 50 μM indomethacin (405268; Sigma-Aldrich, USA), and 5 μg/mL insulin (I3536; Sigma-Aldrich, USA). Cells were incubated at 37°C with 5% CO_2, and the medium was replaced every 2 days[13]. After 14 days, adipogenic differentiation was evaluated using Oil Red O staining per the manufacturer's instructions (C0157S; Beyotime, China). Briefly, cells were fixed with 4% paraformaldehyde (P0099; Beyotime, China) for 20 min at room temperature and stained with Oil Red O working solution (prepared by mixing 3 mL stock with 2 mL diluent) for 30 min, then washed thoroughly with distilled water. Hematoxylin (C0107; Beyotime, China) was applied for 10 min to counterstain nuclei. Stained lipid droplets were imaged using an inverted microscope (CKX53; Olympus, Tokyo, Japan) at ×200 magnification. The percentage of positive-stained area relative to total area was quantified using ImageJ (version 1.47; National Institutes of Health, Bethesda, MD, USA).

Alkaline phosphatase (ALP) staining

After lentiviral transduction, BMSCs were induced to undergo osteogenic differentiation for 14 days. ALP activity was assessed using an ALP chromogenic kit (C3250S; Beyotime, China). Briefly, BCIP/NBT substrate was prepared by mixing 10 μL BCIP solution and 20 μL NBT solution with 3 mL chromogenic buffer. Cells were fixed with 4% paraformaldehyde for 10 min, rinsed with PBS, and incubated with the BCIP/NBT substrate for 30 min at room temperature in the dark. Stained cells (blue-violet) were imaged using an inverted microscope at ×200 magnification. The percentage of positive-stained area relative to total area was quantified using ImageJ (version 1.47; National Institutes of Health, Bethesda, MD, USA).

Alizarin Red S (ARS) Staining

BMSCs subjected to the indicated lentiviral transductions were induced to undergo osteogenic differentiation for 14

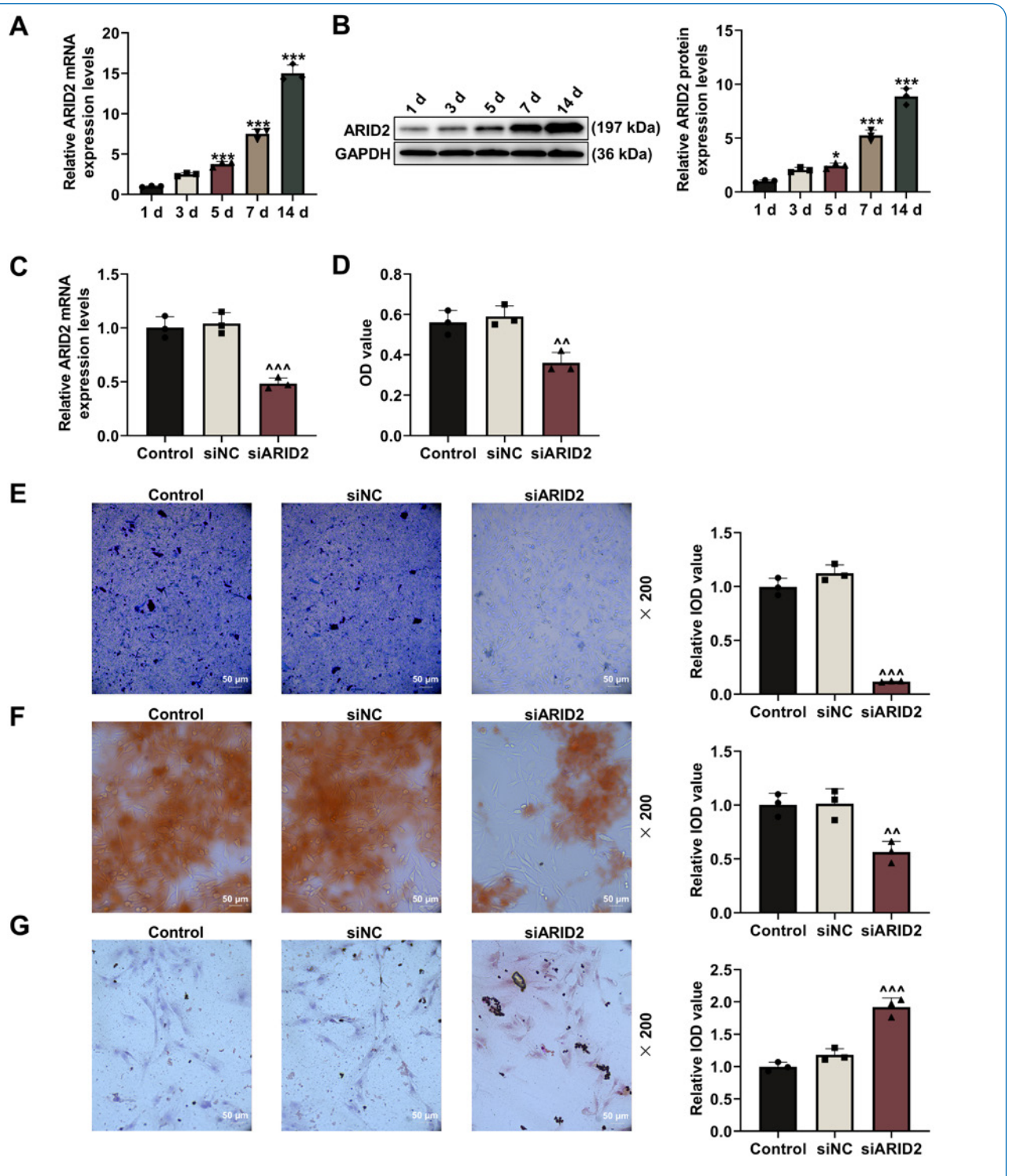

Figure 1. ARID2 expression increased over time in BMSCs undergoing osteogenesis, while ARID2 silencing inhibited proliferation and osteogenesis but favored adipogenesis. (A–B) BMSCs were induced to differentiate into osteoblasts and sampled at 1, 3, 5, 7, and 14 days. ARID2 expression was assessed by qRT-PCR (normalized to GAPDH, reference gene) and western blot (normalized to GAPDH, loading control). (C) ARID2 expression in normally cultured BMSCs after lentiviral ARID2 silencing (siARID2) was measured by qRT-PCR (GAPDH reference). (D) BMSC viability after ARID2 silencing was measured by MTT assay. (E–F) After 14 days of osteogenic induction, ALP activity (ALP staining; ×200, scale bar 50 μm) and mineralized nodule formation (Alizarin Red S staining; ×200, scale bar 50 μm) were evaluated. (G) After 14 days of adipogenic induction, lipid deposition was evaluated by Oil Red O staining (×200, scale bar 50 μm). * P <0.05, *** P <0.001 vs 1 day; ^^ P <0.01, ^^^ P <0.001 vs siNC, n = 3 biological replicates. BMSCs, bone marrow–derived mesenchymal stromal cells; ARID2, AT-rich interactive domain–containing protein 2; qRT-PCR, quantitative reverse-transcription PCR; siARID2, lentivirus-mediated ARID2 silencing; siNC, negative-control lentivirus; OD, optical density.

days. Mineralized matrix deposition was assessed using an osteogenesis assay kit (C0148S; Beyotime, China). Briefly, cells were fixed for 10 min, stained with Alizarin Red S (ARS) solution (pH 4.2) for 30 min at room temperature, and washed thoroughly with distilled water. Mineralized nodules were imaged using an inverted microscope at ×200 magnification. The percentage of positive-stained area relative to total area was quantified using ImageJ (version 1.47; National Institutes of Health, Bethesda, MD, USA).

Western blot

BMSCs (with or without lentiviral transduction) were induced for osteogenic differentiation and lysed in RIPA buffer (89900; Thermo Fisher Scientific, USA) supplemented with a protease and phosphatase inhibitor cocktail (78445; Thermo Fisher Scientific, USA). Total protein concentration was determined using a BCA kit (P0010S; Beyotime, China) according to the manufacturer's instructions. Equal protein amounts (50 μg) were separated by SDS–PAGE (20328ES50; Yeasen, Shanghai, China) and transferred to PVDF membranes (P2438; Sigma-Aldrich, USA). Membranes were blocked with 5% nonfat dry milk in TBST (37573; Thermo Fisher Scientific, USA) for 1 h at room temperature, incubated with primary antibodies (Table 2) overnight at 4°C, washed in TBST, and then incubated with goat anti-rabbit or goat anti-mouse IgG secondary antibodies (Table 2) for 2 h at room temperature. Signals were developed using ECL substrate (1705061; Bio-Rad, Hercules, CA, USA) and captured on an Amersham Imager 600 (GE Healthcare Life Sciences, Pittsburgh, PA, USA). Exposure times (5 s to 2 min) were optimized to keep signals within the linear dynamic range.

For phospho-p65 (p-p65), band intensity was normalized to the corresponding total p65 to account for variation in target abundance. For other targets (ARID2, IκBα), band intensity was normalized to the loading control, GAPDH. Densitometry was performed in ImageJ (version 1.47; National Institutes of Health, Bethesda, MD, USA), and relative expression was calculated as the ratio of target to reference band intensity (target/reference).

Statistical Analysis

GraphPad Prism (version 8.0; GraphPad Software, San Diego, CA, USA) was used for quantitative analyses. Data are presented as mean ± standard deviation (SD) with n = 3 biological replicates per group. Normality and homogeneity of variance were assessed using the Shapiro–Wilk and Brown–Forsythe tests, respectively. Group differences were evaluated by one-way analysis of variance (ANOVA) with Tukey's post hoc test. $P < 0.05$ was considered statistically significant.

Results

ARID2 expression increased during osteogenic induction, whereas its silencing reduced proliferation/osteogenesis and favored adipogenesis in BMSCs

To characterize ARID2 expression during BMSC osteogenic differentiation, BMSCs were induced toward osteogenesis and sampled at 1, 5, 7, and 14 days. Compared with day 1, ARID2 mRNA and protein levels were significantly elevated at days 5, 7, and 14 (Fig. 1A–B; $P < 0.05$). To evaluate function, ARID2 expression was manipulated via lentiviral transduction, which achieved ARID2 silencing (Figure 1C; $P < 0.001$). MTT assays showed that ARID2 silencing decreased BMSC viability (Figure 1D; $P < 0.01$). Osteogenic and adipogenic outcomes were then assessed: ALP and ARS staining revealed reduced ALP activity and mineralized matrix in ARID2-silenced BMSCs undergoing osteogenic induction (Figure 1E–F), whereas Oil Red O staining demonstrated increased lipid accumulation (Figure 1G). Collectively, these findings suggest that ARID2 silencing shifts BMSC differentiation from the osteoblast lineage toward the adipocyte lineage.

STK39 overexpression increased ARID2 expression to encourage BMSC proliferation and osteogenesis

STK39 activates TGF-β1 signaling[11], whose long-term activation downstream of BMP upregulation in MSCs triggers osteolineage commitment and induces ARID2 expression[13]. To determine whether STK39 acts as a positive regulator of ARID2 to favor BMSC osteogenic differentiation, STK39 was overexpressed in BMSCs undertaking osteogenesis. Successful STK39 overexpression in BMSCs was verified by qRT-PCR (Figure 2A; $P<0.001$), and this overexpression persisted when ARID2 was silenced (Figure 2A; $P<0.001$). In BMSCs, ARID2 expression increased upon STK39 overexpression (Figure 2B; $P < 0.001$), which also attenuated transduction-mediated ARID2 silencing (Figure 2B; $P < 0.01$); ARID2 silencing, in turn, reversed the STK39-overexpression–induced ARID2 upregulation (Figure 2B; $P < 0.001$). Furthermore, BMSCs exhibited augmented viability after STK39 overexpression (Figure 2C; $P < 0.01$), whereas viability declined with ARID2 silencing (Figure 2C; $P < 0.05$). STK39 overexpression and ARID2 silencing mutually offset their effects on BMSC viability (Figure 2C; $P< 0.05$). Meanwhile, enhanced ALP activity and mineralized nodule formation were observed in osteogenically differentiating BMSCs when STK39 was overexpressed (Figure 2D–E), and ARID2 silencing attenuated this effect (Figure 2D–E). As anticipated, STK39 overexpression reversed the suppression by ARID2 silencing of ALP activity and mineralized nodule formation in BMSCs undergoing osteogenic differentiation (Figure 2D–E).

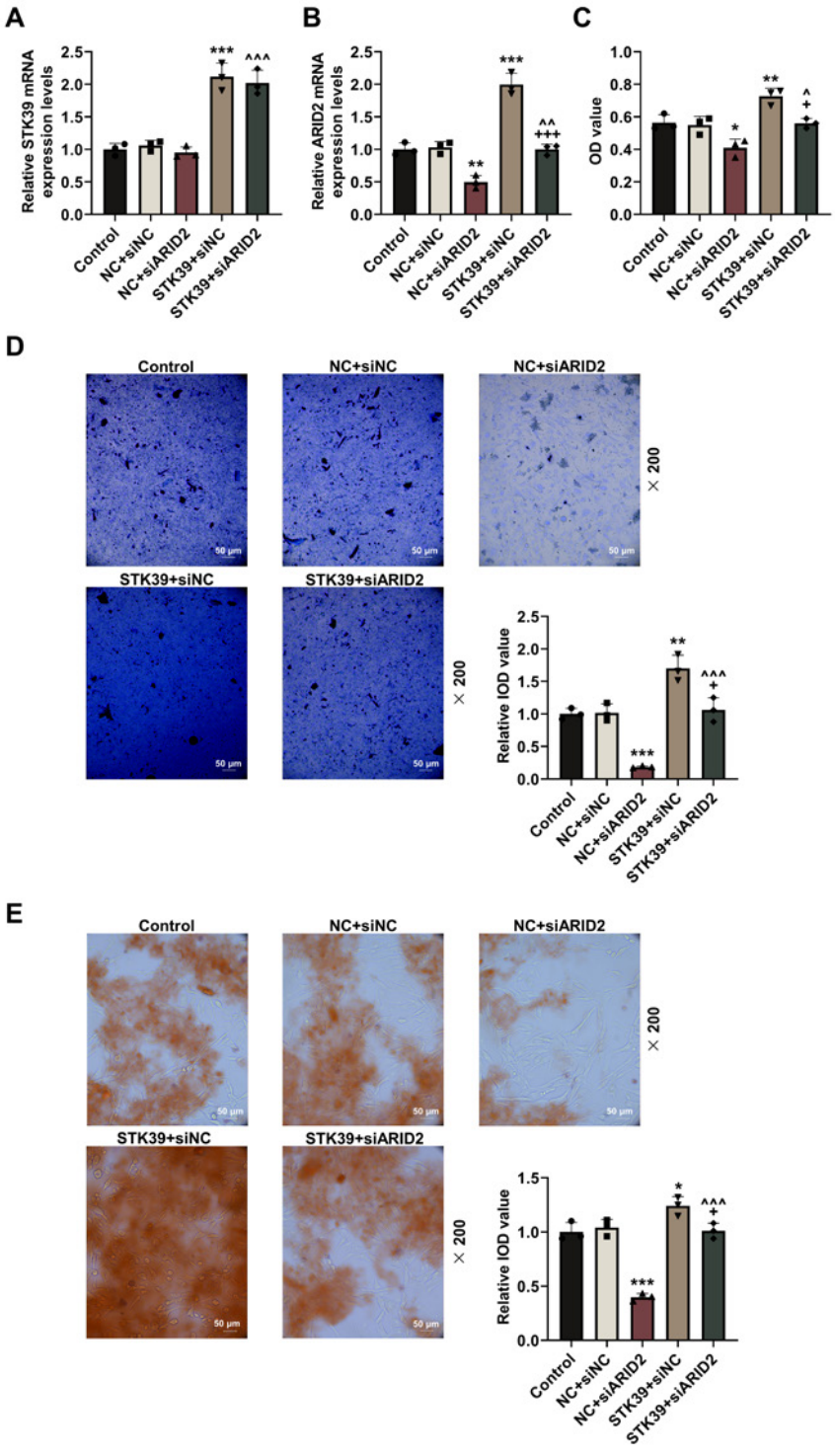

Figure 2. STK39 overexpression increased ARID2 expression to encourage BMSC proliferation and osteogenesis. (A–B) STK39 and ARID2 expression levels in normally cultured BMSCs after transduction with lentiviruses silencing ARID2 (siARID2) and/or lentivirus overexpressing STK39 were assessed by qRT-PCR (normalized to GAPDH). (C) BMSC viability after the indicated transductions was measured by MTT assay. (D–E) BMSCs were transduced as indicated and then subjected to osteogenic induction for 14 days. ALP activity (ALP staining; ×200, scale bar 50 μm) and mineralized nodule formation (Alizarin Red S staining; ×200, scale bar 50 μm) were evaluated. * P <0.05, ** P <0.01, *** P <0.001 vs NC+siNC; ^ P <0.05, ^^ P <0.01, ^^^ P <0.001 vs NC+siARID2; + P <0.05, +++ P <0.001, ⁺ vs STK39+siNC. n = 3 biological replicates. BMSCs, bone marrow–derived mesenchymal stromal cells; STK39, serine/threonine kinase 39; ARID2, AT-rich interactive domain-containing protein 2; qRT-PCR, quantitative reverse-transcription PCR; siARID2, lentivirus-mediated ARID2 silencing; siNC, negative control for ARID2-silencing lentivirus; NC, vector control for STK39 overexpression; OD, optical density.

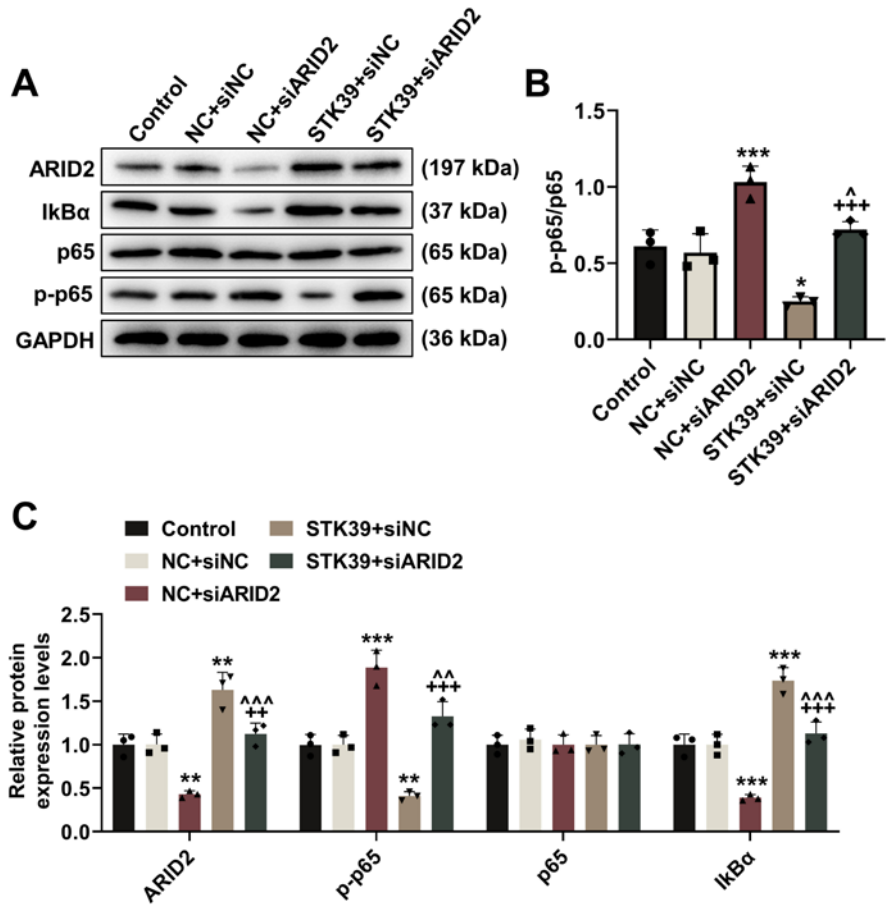

Figure 3. STK39 overexpression increased ARID2 expression and restrained NF-κB signaling in BMSCs undertaking osteogenesis. (A-C) BMSCs were transduced with lentiviruses silencing ARID2 (siARID2) and/or lentivirus overexpressing STK39, then underwent osteogenic differentiation for 14 days. NF-κB pathway–related proteins were assessed by western blot. p-p65 was normalized to total p65; ARID2 and IκBα were normalized to GAPDH. * *P* <0.05, ** *P* <0.01, *** *P* <0.001 vs NC+siNC; ^ *P* <0.05, ^^ *P* <0.01, ^^^ *P* <0.001 vs NC+siARID2; ++ P <0.01, +++ P <0.001 vs STK39+siNC. n = 3 biological replicates. BMSCs, bone marrow–derived mesenchymal stromal cells; STK39, serine/threonine kinase 39; ARID2, AT-rich interactive domain-containing protein 2; siARID2, lentivirus-mediated ARID2 silencing; siNC, negative control for ARID2-silencing lentivirus; NC, vector control for STK39 overexpression; p-p65, phosphorylated p65; NF-κB, nuclear factor κB.

STK39 overexpression increased ARID2 expression and restrained NF-κB signaling in BMSCs undertaking osteogenesis

The involvement of NF-κB signaling in STK39/ARID2–mediated BMSC osteogenic differentiation was examined. In BMSCs undertaking osteogenesis, ARID2 silencing increased the p-p65/p65 ratio and p-p65 levels and decreased ARID2 and IκBα expression, whereas STK39 overexpression drove these readouts in the opposite direction (Figure 3A–C; P< 0.01). STK39 overexpression attenuated the effects of ARID2 silencing, and ARID2 silencing weakened the effects of STK39 overexpression on these NF-κB pathway markers in BMSCs undertaking osteogenesis (Figure 3A–C; P < 0.05). Meanwhile, there was no significant difference in total p65 expression among groups (Figure 3A–C).

Discussion

OP features deterioration of bone mineral density and microarchitecture, leading to compromised bone strength and increased fracture risk; if not treated appropriately, it can trigger a vicious cycle of recurrent fractures[22]. Current pharmacological treatments may have adverse effects, but improved understanding of the cellular events and genetic targets involved in OP progression has contributed

to the development of targeted therapies, which show great promise for OP treatment[5,23]. BMSCs, which possess self-renewal capacity and multilineage differentiation potential, replenish bone tissue and promote bone formation by facilitating osteoblastogenesis, whereas their differentiation into the adipocyte lineage is associated with enhanced osteoclastogenesis during bone remodeling and thus contributes to pathological bone loss, as in OP[24]. This study suggests that STK39 may enhance ARID2 expression and thereby influence the osteogenic–adipogenic balance of BMSCs.

ARID2, a subunit of the PBAF chromatin-remodeling complex, regulates diverse biological processes[25–28], among which development, lineage-specific gene expression, and proliferation appear to be most critically under ARID2 control[28,29]. Prior studies show that the ARID2-containing PBAF complex facilitates osteogenic differentiation of embryonic osteoblasts[30], and recent data indicate that stable ARID2 deletion impairs osteolineage gene expression and compromises osteogenesis in MSCs[13], supporting a pro-osteogenic role for ARID2. Moreover, osteogenic differentiation by BMSCs to maintain bone homeostasis requires substantial metabolic energy[3], while BMSC viability declines with aging, a population prone to OP[1,31]. Consistent with these observations, in our study loss of ARID2 in BMSCs was associated with reduced viability and impaired osteogenic differentiation.

In OP and related pathological conditions, suppressed osteogenic differentiation of BMSCs is often accompanied by promoted adipogenic differentiation, as BMSCs become prone to differentiate into adipocytes rather than osteoblasts under these circumstances[32]. Although prior data reported that osteogenesis impairment caused by ARID2 loss does not co-occur with alterations in adipogenesis[13], other evidence indicates that circulating lipids are associated with DNA methylation of the ARID2 promoter in adipose tissues, tending to repress ARID2 expression[33]. Contrary to that previous report[13], our work found that ARID2 silencing promotes BMSC commitment toward the adipocyte lineage.

STK39, a member of the STE20-like kinase family[34], has been linked to hypertension, autism, Parkinson's disease, and several cancers[35], whereas its association with OP has not been investigated. Reported biological functions of STK39 include regulation of cell proliferation, transformation, differentiation[9], and bone mineralization[10]. Overexpression of STK39 in hepatocellular carcinoma cells activates the TGF-β1–mediated signaling pathway[11], which recruits BMSCs to sites of bone remodeling[4] and promotes their osteogenic differentiation[12], implying that elevated STK39 expression contributes to BMSC osteogenic differentiation—an implication supported by our data. Moreover, induction of ARID2 expression in MSCs is required for long-term BMP/TGF-β signaling–driven osteogenesis[13], which is consistent with a model in which STK39 may influence TGF-β signaling to upregulate ARID2; however, these observations represent an initial mechanistic indication rather than a definitive pathway map, as TGF-β activity was not directly assessed in this study. In line with this expectation, our results showed that STK39 overexpression was accompanied by increased ARID2 expression in BMSCs, and ARID2 silencing attenuated the STK39 overexpression–induced promotion of BMSC osteogenesis, whereas STK39 overexpression in turn partially reversed the inhibitory effect of ARID2 silencing on BMSC osteogenesis—supporting a functional interaction between STK39 and ARID2 rather than definitively establishing a linear upstream–downstream relationship.

NF-κB is a transcription factor known to regulate osteogenic progression, with a context-dependent effect[36]. Nevertheless, most studies report that suppressing NF-κB signaling enhances the osteogenic differentiation of BMSCs and benefits bone regeneration[37–39], whereas activation of NF-κB hinders osteogenesis[17]. In addition to compromising BMSC osteogenesis, NF-κB activation facilitates adipogenic differentiation in BMSCs[17]. Activation of NF-κB requires phosphorylation and consequent degradation of IκBα, after which p65 is phosphorylated and translocates to the nucleus to activate target genes[40]. ARID2 degradation leads to NF-κB (p65) phosphorylation with IκBα downregulation in cervical cancer[18]. Analogously, in our study, ARID2 silencing in osteogenically differentiating BMSCs resulted in p-p65 and IκBα changes consistent with enhanced NF-κB signaling, although global NF-κB activity (e.g., reporter assays or nuclear translocation) was not directly assessed.

STK39 perturbation has also been reported to modulate NF-κB signaling in a context-dependent manner, with effects that include changes in IκBα degradation and p65 phosphorylation[41,42]. These NF-κB-related findings should be interpreted as preliminary, suggesting a potential interaction among STK39, ARID2, and NF-κB signaling rather than demonstrating a fully mapped regulatory cascade.

In this study, we used the immortalized human BMSC line UE6E7T-1. Immortalization by HPV16 E6/E7 and hTERT confers an extended proliferative lifespan, which is advantageous for experimental reproducibility. However, potential impacts of this modification should be considered. The HPV16 E6/E7 oncoproteins can inactivate the tumor suppressors p53 and pRb, potentially altering baseline proliferation and differentiation pathways compared with primary BMSCs[43]. With respect to NF-κB signaling, HPV E6 has been reported to interact with and potentially modulate NF-κB activity[44,45], which may influence the basal state of this pathway in UE6E7T-1 cells. Nonetheless, this well-characterized line retains fundamental BMSC properties, including differentiation capacity[19,46], and is widely used for mechanistic studies in mesenchymal stem-cell biology. Given these considerations, the present work should be viewed as an *in vitro* proof-of-concept rather than a definitive mechanistic demonstration. Future studies using primary human BMSCs, animal models, and *in vivo* validation will be essential to determine the translational relevance of the STK39–ARID2 axis in OP.

Conclusion

In conclusion, our results suggest a potential role for STK39 in BMSC osteogenesis: STK39 overexpression was associated with increased ARID2 expression and reduced NF-κB activity, which together may influence the osteogenic–adipogenic balance of BMSCs. Accordingly, STK39 overexpression (and the STK39–ARID2 axis) may represent a promising molecular target for OP; however, further validation in primary human BMSCs and *in vivo* models will be essential before therapeutic translation.

Ethics approval

This study involved only an established, commercially available human BMSC line (UE6E7T-1; JCRB1131) and did not include human participants, identifiable personal data, or animal experiments; therefore, formal ethics committee/IRB or animal ethics approval was not required under institutional policies.

Authors' contributions

Study concept and design: YW, LZ; Analysis and interpretation of data: DW, ZNC; Drafting of the manuscript: YW, LZ; Critical revision of the manuscript for important intellectual content: YW, LZ; Statistical analysis: DW, ZNC; Study supervision: YW, LZ. All authors have read and approved the manuscript.

References

1. Johnston CB, Dagar M. Osteoporosis in older adults. Med Clin North Am. 2020;104(5):873–884.
2. Reid IR, Billington EO. Drug therapy for osteoporosis in older adults. Lancet. 2022;399(10329):1080–1092.
3. Ning K, Liu S, Yang B, et al. Update on the effects of energy metabolism in bone marrow mesenchymal stem cells differentiation. Mol Metab. 2022;58:101450.
4. Crane JL, Cao X. Bone marrow mesenchymal stem cells and TGF-β signaling in bone remodeling. J Clin Invest. 2014;124(2):466–472.
5. Aibar-Almazán A, Voltes-Martínez A, Castellote-Caballero Y, et al. Current status of the diagnosis and management of osteoporosis. Int J Mol Sci. 2022;23(16):9465.
6. Jiang Y, Zhang P, Zhang X, et al. Advances in mesenchymal stem cell transplantation for the treatment of osteoporosis. Cell Prolif. 2021;54(1):e12956.
7. Hu L, Yin C, Zhao F, Ali A, Ma J, Qian A. Mesenchymal Stem Cells: Cell Fate Decision to Osteoblast or Adipocyte and Application in Osteoporosis Treatment. Int J Mol Sci. 2018;19(2):360.
8. Gagnon KB, Delpire E. Two Ste20-Related Protein Kinases Regulating Ion Transport. Physiol Rev. 2012;92(4):1577–1617.
9. Johnston AM, Naselli G, Gonez LJ, et al. SPAK, a STE20/SPS1-related kinase that activates the p38 pathway. Oncogene. 2000;19(37):4290–4297.
10. Pathare G, Föller M, Michael D, et al. Enhanced FGF23 serum concentrations and phosphaturia in gene-targeted mice expressing WNK-resistant SPAK. Kidney Blood Press Res. 2012;36(1):355–364.
11. Wang J, Fan Z, Li J, et al. Transcription factor specificity protein 1-mediated serine/threonine kinase 39 upregulation promotes the proliferation, migration, invasion and epithelial–mesenchymal transition of hepatocellular carcinoma cells by activating the transforming growth factor-β1/Smad2/3 pathway. Bioengineered. 2021;12(1):3566–3577.
12. Li J, Ge L, Zhao Y, et al. TGF-β2 and TGF-β1 differentially regulate the odontogenic and osteogenic differentiation of mesenchymal stem cells. Arch Oral Biol. 2022;135:105357.
13. Sinha S, Biswas M, Chatterjee SS, et al. Pbrm1 steers mesenchymal stromal cell osteolineage differentiation by integrating PBAF-dependent chromatin remodeling and BMP/TGF-β signaling. Cell Rep. 2020;31(4):107570.
14. Vicent GP, Zaurin R, Nacht AS, et al. Two chromatin remodeling activities cooperate during activation of hormone responsive promoters. PLoS Genet. 2009;5(7):e1000567.
15. Yan Z, Cui K, Murray DM, et al. PBAF chromatin-remodeling complex requires a novel specificity subunit, BAF200, to regulate expression of selective interferon-responsive genes. Genes Dev. 2005;19(14):1662–1667.
16. Yu J, Shen L, Liu Y, et al. The m6A methyltransferase METTL3 cooperates with demethylase ALKBH5 to regulate osteogenic differentiation through NF-κB signaling. Mol Cell Biochem. 2020;463(1–2):203–210.
17. Lin H, Liu T, Li X, et al. The role of gut microbiota metabolite trimethylamine N-oxide in functional impairment of bone marrow mesenchymal stem cells in osteoporosis disease. Ann Transl Med. 2020;8(16):1009.
18. Li H, Chi X, Li R, et al. HIV-1-infected cell-derived exosomes promote the growth and progression of cervical cancer. Int J Biol Sci. 2019;15(11):2438–2447.
19. Takeda Y, Mori T, Imabayashi H, et al. Can the life span of human marrow stromal cells be prolonged by bmi-1, E6, E7, and/or telomerase without affecting cardiomyogenic differentiation? J Gene Med. 2004;6(8):833–845.
20. Bougioukli S, Sugiyama O, Pannell W, et al. Gene therapy for bone repair using human cells: superior osteogenic potential of bone morphogenetic protein 2-transduced mesenchymal stem cells derived from adipose tissue compared to bone marrow. Hum Gene Ther. 2018;29(4):507–519.
21. Livak KJ, Schmittgen TD. Analysis of relative gene expression data using real-time quantitative PCR and the 2(−ΔΔCT) method. Methods. 2001;25(4):402–408.
22. LeBoff MS, Greenspan SL, Insogna KL, et al. The clinician's guide to prevention and treatment of

osteoporosis. Osteoporos Int. 2022;33(10):2049–2102.
23. Song S, Guo Y, Yang Y, et al. Advances in pathogenesis and therapeutic strategies for osteoporosis. Pharmacol Ther. 2022;237:108168.
24. Yu W, Liu X, Guo X, et al. Bone marrow adipogenic lineage precursors promote osteoclastogenesis in bone remodeling and pathologic bone loss. J Clin Invest. 2021;131(2):e140214.
25. Loesch R, Chenane L, Colnot S. ARID2 chromatin remodeler in hepatocellular carcinoma. Cells. 2020;9(10):2152.
26. He L, Tian X, Zhang H, et al. BAF200 is required for heart morphogenesis and coronary artery development. PLoS One. 2014;9(10):e109493.
27. Zhang X, Azhar G, Zhong Y, et al. Zipzap/p200 is a novel zinc finger protein contributing to cardiac gene regulation. Biochem Biophys Res Commun. 2006;346(3):794–801.
28. Kortschak RD, Tucker PW, Saint R. ARID proteins come in from the desert. Trends Biochem Sci. 2000;25(6):294–299.
29. Patsialou A, Wilsker D, Moran E. DNA-binding properties of ARID family proteins. Nucleic Acids Res. 2005;33(1):66–79.
30. Xu F, Flowers S, Moran E. Essential role of ARID2 protein-containing SWI/SNF complex in tissue-specific gene expression. J Biol Chem. 2012;287(7):5033–5041.
31. Li X, Wang X, Zhang C, et al. Dysfunction of metabolic activity of bone marrow mesenchymal stem cells in aged mice. Cell Prolif. 2022;55(3):e13191.
32. Ouyang Z, Kang D, Li K, et al. DEPTOR exacerbates bone-fat imbalance in osteoporosis by transcriptionally modulating BMSC differentiation. Biomed Pharmacother. 2022;151:113164.
33. Rönn T, Perfilyev A, Jonsson J, et al. Circulating triglycerides are associated with human adipose tissue DNA methylation of genes linked to metabolic disease. Hum Mol Genet. 2023;32(11):1875–1887.
34. Ramoz N, Cai G, Reichert JG, et al. An analysis of candidate autism loci on chromosome 2q24–q33: evidence for association to the STK39 gene. Am J Med Genet B Neuropsychiatr Genet. 2008;147B(7):1152–1158.
35. Huang T, Zhou Y, Cao Y, et al. STK39, overexpressed in osteosarcoma, regulates osteosarcoma cell invasion and proliferation. Oncol Lett. 2017;14(4):4599–4604.
36. Kaltschmidt C, Greiner JFW, Kaltschmidt B. The transcription factor NF-κB in stem cells and development. Cells. 2021;10(8):2042.
37. Wang F, Wang W, Kong L, et al. Accelerated bone regeneration by adrenomedullin 2 through improving the coupling of osteogenesis and angiogenesis via β-catenin signaling. Front Cell Dev Biol. 2021;9:649277.
38. Wang YJ, Zhang HQ, Han HL, et al. Taxifolin enhances osteogenic differentiation of human bone marrow mesenchymal stem cells partially via NF-κB pathway. Biochem Biophys Res Commun. 2017;490(1):36–43.
39. Chang J, Liu F, Lee M, et al. NF-κB inhibits osteogenic differentiation of mesenchymal stem cells by promoting β-catenin degradation. Proc Natl Acad Sci U S A. 2013;110(23):9469–9474.
40. Yu H, Lin L, Zhang Z, et al. Targeting NF-κB pathway for the therapy of diseases: mechanism and clinical study. Signal Transduct Target Ther. 2020;5(1):209.
41. Hung CM, Peng CK, Yang SS, et al. WNK4-SPAK modulates lipopolysaccharide-induced macrophage activation. Biochem Pharmacol. 2020;171:113738.
42. Wu SW, Peng CK, Wu SY, et al. Obesity attenuates ventilator-induced lung injury by modulating the STAT3–SOCS3 pathway. Front Immunol. 2021;12:720844.
43. Wiest T, Schwarz E, Enders C, et al. Involvement of intact HPV16 E6/E7 gene expression in head and neck cancers with unaltered p53 status and perturbed pRb cell cycle control. Oncogene. 2002;21(10):1510–1517.
44. Jin Y, Li Y, Wang X, et al. Secretory leukocyte protease inhibitor suppresses HPV E6-expressing HNSCC progression by mediating NF-κB and Akt pathways. Cancer Cell Int. 2019;19:220.
45. An J, Mo D, Liu H, et al. Inactivation of the CYLD deubiquitinase by HPV E6 mediates hypoxia-induced NF-κB activation. Cancer Cell. 2008;14(5):394–407.
46. Mori T, Kiyono T, Imabayashi H, et al. Combination of hTERT and bmi-1, E6, or E7 induces prolongation of the life span of bone marrow stromal cells from an elderly donor without affecting their neurogenic potential. Mol Cell Biol. 2005;25(12):5183–5195.